

# Normal stress-induced permeability hysteresis of a fracture in a granite cylinder

A. P. S. SELVADURAI\*

*Department of Civil Engineering and Applied Mechanics, McGill University, Montréal, QC, Canada*

## ABSTRACT

The paper examines the influence of axial stress-induced closure of a fracture on its permeability. The experiments were conducted on a cylinder of Barre Granite measuring 457 mm in diameter and 510 mm in height, containing a central cylindrical cavity of diameter 75 mm. Radial flow hydraulic pulse tests were conducted in a previous research investigation (Selvadurai *et al.*, PAGEOPH, 2005) to determine the permeability characteristics of the intact granite. In the continuation of the research, a fracture was introduced in the cylinder with its nominal plane normal to the axis of the cylinder. Axial compressive stress was applied normal to the plane of the fracture. An increase in the compressive normal stress acting on the fracture caused a reduction in the aperture of the fracture, which resulted in the reduction in its permeability. Steady state radial flow tests were conducted on the fractured axially stressed sample to determine the variation of fracture permeability with axial normal stress. The analytical developments also take into account flow through the matrix region as the normal stress increases. The results of the experimental investigations indicate that the complete stress relief of a fracture previously subjected to a normal stress of 7.5 MPa can result in a permeability increase of approximately three orders of magnitude. These findings are relevant to shallow depth geotechnical construction activities where enhanced fluid flow can be activated by stress relief. As the fracture aperture closes with high normal stress, the flow through the matrix can be appreciable and if this factor is not taken into consideration the interpretation of fracture permeability can be open to error. This factor can be of interest to the interpretation of permeability of fractures in deep crustal settings where the stresses acting normal to the fracture surface can inhibit flow in the fracture.

Key words: axially stressed fractures, flow in fractures, permeability hysteresis, stress-induced fracture closure

Received 29 January 2014; accepted 26 August 2014

Corresponding author: A. P. S. Selvadurai, Department of Civil Engineering and Applied Mechanics, McGill University 817 Sherbrooke Street West, Montréal, QC, H3A 0C3, Canada.

Email: patrick.selvadurai@mcgill.ca. Tel: +1 514 398 6672. Fax: +1 514 398 7361.

*Geofluids* (2015) 15, 37–47

## INTRODUCTION

Fractures are geological features that can dominate the fluid transport characteristics of geologic media. Fractures are important to groundwater hydrology, environmental earth science and, particularly, environmental geomechanics problems associated with energy resources recovery from gas bearing shales, geologic sequestration of greenhouse gases and deep geologic disposal of hazardous material including heat-emitting radioactive wastes. The literature covering these areas is vast, and no attempt will be made to provide a comprehensive literature review. Articles covering these top-

ics and those with specific relevance to the role of fractures on the containment strategy are given by Noorishad *et al.* (1984), Boulon *et al.* (1993); Selvadurai & Nguyen (1995, 1997), Nguyen & Selvadurai (1995, 1998), Rutqvist & Tsang (2002), Chan *et al.* (2005) and Selvadurai & Yu (2005). The importance of fractures and other defects will invariably depend on the scale at which such defects enter the description of the flow processes in naturally occurring geological media. For example, in laboratory scale testing of granitic rocks, the fractures can be intergranular cracks in the three major minerals, coincident grain boundary cracks and trans-granular cracks. In contrast, at regional scales the fractures are largely well defined, distinct defects with geometrical characteristics that enable the definition of features such as gouge, debris fill, etc., that can be treated as separate

\*William Scott Professor and James McGill Professor

material regions. An intermediate scale can refer to conditions that can be encountered at a fracture intersecting a borehole and packer system installed for measurement of hydraulic properties. A hydraulically created fracture will, in general, involve originally nearly mated surfaces; these can experience either closure, opening or relative movement depending on the state of stress existing in the vicinity of the borehole. The scale of the problem is such that a typical situation involving a borehole intersecting a fracture can be investigated at near field scale in the laboratory. Investigations involving both laboratory and field determination of the permeability of mechanically inactive or stationary fractures are numerous and references to these studies can be found in the volumes and articles by Snow (1968), Louis (1974), Raven & Gale (1985), Gale (1990), Makurat *et al.* (1990a,b), Boulon *et al.* (1993), Yeo *et al.* (1998), Pyrak-Nolte & Morris (2000), Bart *et al.* (2004), Hans & Boulon (2003), Sausse & Genter (2005), Selvadurai *et al.* (2005), Giacomini *et al.* (2007) and Selvadurai & Selvadurai (2010).

A striking feature in the modelling of fractures in a hydrogeological context is that, by and large, the fractures are treated as stationary features that experience no response to either mechanical or thermal phenomena or changes to the fluid pressure. This is at variance with the well established approaches in geomechanics of rocks where response of the fracture to mechanical effects and failure is generally the norm in terms of modelling the mechanical performance of the fracture. The earliest investigations in this area are due to Patton (1966) who conducted experiments on artificial fractures, and the focus was primarily on evaluating the strength of the joint. Processes such as dilatancy during shear, which can contribute to drastic alterations in the permeability of fractures, were left uninvestigated. The investigations by Ladanyi & Archambault (1970), Jaeger (1971), Barton & Choubey (1977) and Bandis *et al.* (1983) proposed strength criteria which were departures from the bi-linear form of the shear strength criterion for the fracture. A great deal of attention has been focused on the mechanical characterization of the performance of the fracture, and these efforts are also described in the literature (Selvadurai & Boulon 1995; Nguyen & Selvadurai 1998; Jafari *et al.* 2004). Permeability alterations during shear were investigated by Witherspoon *et al.* (1979), Barton (1982), Elliot *et al.* (1985), Benjelloun (1993) and Adler (1997). The work of Nguyen & Selvadurai (1998) dealing with dilatant fractures, builds on the model proposed by Plesha (1987), incorporating the influences not only of empirical relationships based on commonly used fracture topography measures such as the *Joint Roughness Coefficient* (JRC) and *Joint Compressive Strength* (JCS) but also a mathematically consistent elasto-plasticity model that accounts for asperity degradation (Makurat *et al.* 1990a,b). The transformation of asperity degradation in fractures to gouge development, which

ultimately has a significant influence on mechanically induced alterations to the permeability of fractures, requires alternative approaches that can involve continuum to discrete transformation of a fracture zone and continual degradation of the fragments with mechanical action (Selvadurai & Boulon 1995; Selvadurai & Sepehr 1999a,b; Selvadurai 2009; Massart & Selvadurai 2012, 2014). Such procedures, without provision for a proper algorithm that transforms a continuum region to a discrete system, will be of marginal value to modelling gouge development in fractures. Recent investigations of the influence of permeability evolution during stressing of rocks have been prompted by an interest in identifying the development of excavation damage zones around opening that are planned for the deep geologic disposal of heat-emitting radioactive wastes (Hudson *et al.* 2008; Nguyen & Jing 2008; Rejeb *et al.* 2008; Rutqvist *et al.* 2008; Najari & Selvadurai, 2014; Liu *et al.* 2013). The evolution of micro-mechanical damage in rocks and the consequent alteration in the deformability characteristics have been documented by Zoback & Byerlee (1975), Shiping *et al.* (1994) and Kiyama *et al.* (1996) but the extension of the concepts to permeability evolution is largely theoretical (Mahyari & Selvadurai 1998; Selvadurai 2004; Selvadurai & Shirazi 2004, 2005). Recent investigations by Shao *et al.* (1999), Souley *et al.* (2001), Zhou *et al.* (2006), Hu *et al.* (2010) and Massart & Selvadurai (2012) have developed permeability evolution concepts that match experimental data derived from testing of rock cores. Other examples of permeability evolution, particularly under isotropic compression, have been discussed by several investigators including Zhu & Wong (1997), Selvadurai & Glowacki (2008), Selvadurai *et al.* (2011) and Selvadurai & Jenner (2012). In these studies, the emphasis is on micro-mechanical defect generation under complex stress states, which contributes to either permeability enhancement or permeability reduction depending on the state of stress.

Investigations that examine the influence of stress states on the permeability characteristics of fractures are rare. Major obstacles for incorporating the influences of mechanical actions on the fluid transport characteristics of fractures can arise from the following: (i) the size of samples or scale effects that are representative of the fractures (Witherspoon *et al.* 1979), (ii) the precise identification of the alteration in the stress states relevant to problems in hydro-geomechanics (Haimson 1975; Stephansson 1985; Ingebritsen *et al.* 2006), (iii) the physical arrangements of a test large enough to apply, with a degree of control, the variety of relative motions that can result from alterations in the ambient stress state, (iv) the development of sound experimental procedures that can be used to observe permeability alterations in the fracture regions as the stress state is altered and (iv) the relationship of the evolving permeability to processes such as fracture closure and

gouge generation, particularly as a function of the attainment of the failure threshold in regions of the fracture. Simultaneous consideration of all these factors is an almost impossible task in experimental geomechanics research and to date attention has focused on extremely small scale investigations that may not completely capture the *in situ* characteristics of fractures at scales of interest to hydro-geomechanical applications.

This paper presents the results from a series of fracture flow experiments conducted on a large cylinder of Barre Granite measuring 457 mm in diameter and 510 mm in height containing a 57 mm diameter cylindrical cavity located at the centre of the cylinder over its entire height (Fig. 1). To the author's knowledge, this is one of the few instances where a large cylinder of the scale indicated has been used in a laboratory experiment. The experimental facility was designed in such a way that transient radial flow pulse tests could first be conducted on the intact cylinder through pressurization of the central borehole. In a previous study (Selvadurai *et al.* 2005), the experimental facility was used to determine the intact permeability of the Barre Granite, which corresponds to the matrix permeability of the material. In this paper, we consider the situation where the cylinder contains a fracture at a central plane perpendicular to its axis. The alteration in the permeability of the fracture due to an axial normal stress is determined by conducting steady state radial flow experiments. The influence of the radial flow through the intact segments of the frac-

tured cylinder is included in calculation of the fracture permeability.

## THEORETICAL ASPECTS

### Radial flow hydraulic pulse testing of the intact cylinders

The theoretical background and modelling of the radial flow hydraulic pulse tests conducted on the intact Barre Granite was presented by Selvadurai *et al.* (2005). The conventional approach for estimating the permeability from hydraulic pulse tests relies on the piezo-conduction equation, and derivations of the equations are given in standard texts (Bear 1972; Philips 1991; Selvadurai 2000; Ichikawa & Selvadurai 2012). The pressure transients are assumed to occur in a fluid-saturated porous medium that can be described by the classical theory of poroelasticity proposed by Biot (1941) (see also Selvadurai & Yue 1994; Selvadurai 1996, 2007) that takes into account the coupling between the deformations of the porous skeleton and the compressible pore fluid. In conventional treatments of hydraulic pulse tests, it is implicitly assumed that the pressure transients can be described by the uncoupled piezo-conduction equation, which accounts for the compressibility of the pore fluid, the compressibility of the porous skeleton and the compressibility of the material constituting the porous fabric. A comparison between results for the one-dimensional hydraulic pulse test derived from the piezo-conduction equation, and Biot's theory of poroelasticity was performed by Wang (2000) and generally, the results for the two approaches compare favourably for low permeability materials. More recently, Selvadurai & Najari (2013) conducted similar studies and arrived at the conclusion that the piezo-conduction equation can be used satisfactorily for estimating the permeability characteristics of low permeability materials such as Westerly Granite, Indiana Limestone and Stanstead Granite from Quebec, Canada. The simplest analytical result that can be used to interpret two-dimensional axisymmetric radial flow hydraulic pulse tests assumes that the pulse test is conducted in a cylindrical cavity located in a fluid-saturated porous medium of infinite extent. Selvadurai & Carnaffan (1997) have investigated the validity of this assumption particularly when hydraulic pulse tests are conducted in annular fluid-saturated regions and provide constraints that allow the application of the theoretical results to infinite domains. The influence of air voids within the pressurized cavity on the interpretation of the conventional hydraulic pulse test was examined more recently by Selvadurai & Ichikawa (2013). Avoiding details, it can be shown that the pressure decay in a fluid-filled cylindrical cavity located in a fluid-saturated porous medium due to transient radial flow in the infinite region is given by

$$p(t) = p_0 \exp(4\alpha\beta) \operatorname{erfc}(2\sqrt{\alpha\beta}) \quad (1)$$

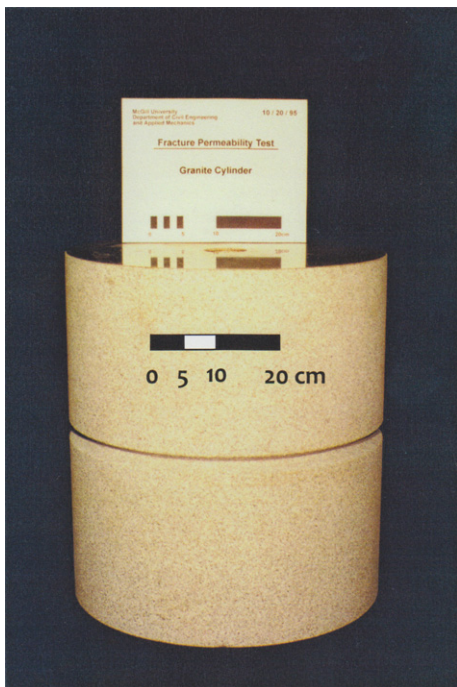


Fig. 1. The cylindrical sample of the Barre Granite used in the experimental investigations. Cylindrical sample containing the V-notch for creation of fracture [After Selvadurai *et al.* (2005)]

In (1)  $p(r,t)$  is the transient pressure potential in the porous region,  $t$  is the time variable,  $r$  is the radial coordinate,  $\text{erfc}(x)$  is the complementary error function,  $p_o$  is the initial pressure, and

$$\alpha = \left( \frac{\pi a^2 S}{V_w C_w \gamma_w} \right); \beta = \left( \frac{\pi T_R t}{V_w C_w \gamma_w} \right) \quad (2)$$

where

$$S = l\gamma_w(nC_w + C_{eff}); T_R = k_i l = K_i l \gamma_w \eta \quad (3)$$

Also, in (2) and (3),  $S$  is the storage coefficient (nondimensional);  $T_R$  is the transmissivity of the cylinder of height  $l$  ( $L^2/T$ );  $n$  is the porosity (nondimensional);  $C_w$  is the compressibility of the pore water ( $LT^2/M$ );  $C_{eff}$  is the compressibility of the porous skeleton ( $LT^2/M$ );  $K_i$  is the permeability of the intact rock ( $L^2$ );  $k_i$  is the hydraulic conductivity of the intact rock ( $L/T$ );  $V_w$  is the volume of the pressurized region ( $L^3$ );  $\eta$  is the dynamic viscosity ( $M/LT$ ); and  $\gamma_w$  is the unit weight of the fluid ( $M/L^2T^2$ ).

Hydraulic pulse tests conducted previously by Selvadurai *et al.* (2005) estimate that the permeability of the intact granite is between  $0.40 \times 10^{-18} \text{ m}^2$  and  $1.20 \times 10^{-18} \text{ m}^2$ . Steady state flow tests conducted on the intact cylinder gave values that ranged from  $1.21 \times 10^{-18} \text{ m}^2$  to  $1.46 \times 10^{-18} \text{ m}^2$ . Considering these ranges, the permeability of the intact granite is taken to be approximately  $1.20 \times 10^{-18} \text{ m}^2$

### Radial steady flow testing of fractured cylinders

In this series of experiments, the intact granite cylinder containing the central cavity was fractured by diametral compression along a pre-cut groove located on the outer surface of the cylinder (Fig. 1). The fracture is obtained by inducing a near tensile stress field at a diametral plane. When dealing with gouge-free plane fractures, the issue of fracture topography, fracture roughness etc., and their influences on the fluid transport characteristics have been investigated extensively in the literature (Raven & Gale 1985; Cook 1992; Pyrak-Nolte & Morris 2000; Méheust & Schmittbuhl 2003). The objective, here, is to use the parallel plate analogue as an elementary model and to establish the pattern of reduction in the permeability of the fracture as the stress normal to the fracture plane is subjected to quasi-static stress cycling. Considering the parallel plate model and fluid flow through the fracture with an aperture  $2\lambda$ , it can be shown that

$$K_f = \frac{\eta Q_f \log_e(b/a)}{4\pi \lambda (p_a - p_b)} [Units(length)^2] \quad (4)$$

where  $Q_f$  is the flow rate through the fracture ( $L^3/T$ ),  $b$  is the external radius of the fracture ( $L$ ); and  $p_a$  and  $p_b$  are the hydraulic fluid pressures ( $M/LT^2$ ) at the inner and outer boundaries of the fracture. (Considering the

overflow locations shown in Fig. 2, the fluid pressure at the outer boundary of the fracture will be maintained at nearly atmospheric pressure.) As the axial stresses increase, the fracture aperture will be reduced and the flow through the intact matrix can influence the flow process, although the flow rate measured in the steady state flow experiment is the combined flow rate  $Q$  occurring through both the intact region and the fracture. Because the pulse testing of the intact cylinder provides an estimate for the matrix permeability  $K_i$  we obtain the following result for the permeability of the fracture ( $K_f^I$ ) that also accounts for the fluid flow through the intact matrix:

$$K_f^I = \left( \frac{\eta Q \log_e(b/a)}{4\pi\sqrt{3}(p_a - p_b)} - \frac{K_i l}{2\sqrt{3}} \right)^{2/3} [Units(length)^2] \quad (5)$$

These results can be used to examine the influence of matrix flow in accurately interpreting the permeability of a fracture that is subjected to a stress normal to its plane.

As the magnitude of  $K_i l$  becomes small in comparison to the first term on the right hand side of (5), the permeability of the fracture can be calculated using the result (4), where

$$\lambda = \left( \frac{3\eta Q \log_e(b/a)}{8\pi(p_a - p_b)} \right)^{1/3} [Units(length)] \quad (6)$$

The permeability of the fracture can be represented by the parallel plate model (Selvadurai 2000) where

$$K_f = \frac{(2\lambda)^2}{12} [Units(length)^2] \quad (7)$$

The permeability of *relatively open fractures* ( $K_f^{II}$ ) can be obtained from the result

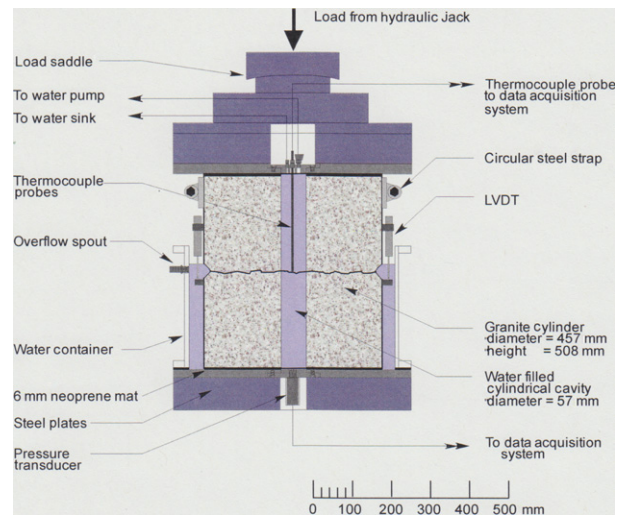


Fig. 2. Detail of the experimental arrangements for application of external loads and for the pressurization of the central fluid-filled cavity.

$$K_f^{II} = \left( \frac{\eta Q \log_e(b/a)}{4\pi\sqrt{3}(p_a - p_b)} \right)^{2/3} [Units(length)^2] \quad (8)$$

which is the expression obtained when  $K_i$  is set to zero in (5).

## EXPERIMENTAL PROCEDURES

Aspects of the experimental investigations dealing with hydraulic pulse testing of the Barre Granite are documented by Selvadurai *et al.* (2005). A petrographic analysis conducted by Hardy (1991) indicates that the Barre Granite, a blue-grey granodiorite, contains approximately 23% quartz, 61% feldspar and 11% micas. The large diameter cylindrical samples of the Barre Granite used in the experimental investigations were obtained from Vermont, USA. The mechanical and physical properties of the granite were determined from ASTM and ISRM Standard Tests. [These results are summarized in Table 1 of Selvadurai *et al.* (2005).] Diametral compression was then used to create the fracture. The V-notch ensured that the fracture plane was nominally perpendicular to the axis of the cylinder. The plane ends of the cylinder were machine polished to a mirror finish (Fig. 1) by the suppliers to ensure parallel end planes that could be mechanically sealed both during the transient pulse tests and the steady state fracture permeability tests.

The details of the test frame used to apply stresses normal to the plane of the fracture are described by Selvadurai *et al.* (2005). Separate stainless steel plates of thickness 25 mm were provided at the plane ends of the cylinder to prevent corrosion of the loading plates in the event of water leakage from the pressurized central cavity. The stainless steel plates were also fitted with O-rings to provide an adequate seal during pressurization of the central cavity. The effectiveness of this sealing technique was verified by pressurization of a hollow stainless steel cylinder, which maintained the pressure without loss (except for fluctuations of ambient temperatures) for a period of 8 days. Neoprene mats (thickness 6 mm) were also provided at the upper and lower contact surfaces to minimize any stress concentrations that could occur due to uneven contact between the test cylinder and the stainless steel plates. The stainless steel plates contained specially designed couplings to provide access to sensors and instrumentation within the fluid-filled cavity. The stainless steel base plate incorporated a pressure transducer (maximum pressure of 2.07 MPa) to measure fluid pressure. The upper stainless steel plate contained a specially designed coupling unit that provided access for the inlet and outlet water supply ports. A thermocouple located in this coupling was used to measure water temperature in the cavity during the tests. All inlet and outlet leads for water supply were made of stainless steel, and Swagelok valves

(maximum pressure rating of 20.7 MPa) were used to seal the fluid pressure in the cavity during hydraulic pulse tests on the intact sample. The compression of the intact sample during application of sealing stresses was found to be negligible. During permeability testing of fractures, however, the lower stainless steel plate was incorporated with a Plexiglas reservoir to collect any fluid migrating through the fracture (Fig. 2). Testing of fracture permeability also required measurement of the closure of the fracture during application of axial stresses. Three linear variable differential transformers (LVDTs) (Fig. 3), located at orientations of  $120^\circ$  around the circumference of the cylinder, were used to measure closure of the fracture. The three values were averaged to arrive at the closure of the fracture during the application of axial stress. A schematic detail of the sample and test arrangement used when performing steady radial flow tests through the fracture is shown in Fig. 4. The experimental facilities also included a Shimadzu precision pump for saturating the granite cylinder, for applying the pressure pulse required to conduct the hydraulic pulse tests and for maintaining a steady flow when conducting permeability tests on the fractured cylinder. The data sets from all the experiments were recorded with a computerized data acquisition system that uses LabView Data Processing.

Prior to fracturing the granite cylinder, four markers (Demec Gauges) were installed on the surface of the cylinder to allow re-assembly of the split specimen at the correct orientation (Fig. 5) and for the measurement of the fracture aperture prior to the application of normal stresses. In the central cavity of the granite cylinder, a steel bar was secured with end plates and rubber pads to allow axial expansion during splitting about a plane normal to the axis of the cylinder but to prevent relative movements between the separate parts of the fractured cylinder, which could lead to unwanted asperity shear. Splitting action was initiated by applying point loads through hardened steel wedge shaped regions. The plane of the fracture can exhibit an uneven configuration depending upon the microstructural fabric of the granite. The provision of the mid-plane groove localized the plane of failure, but where the groove

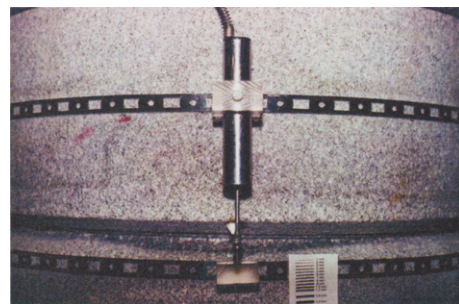


Fig. 3. The LVDT arrangement for movements of the fracture.

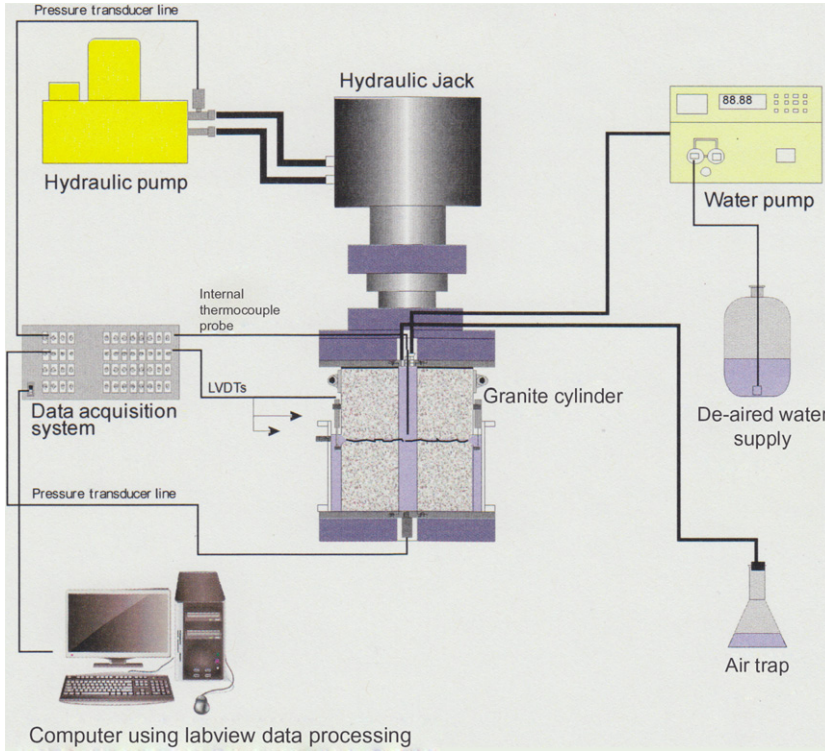


Fig. 4. Schematic view of the radial flow permeability testing arrangement.

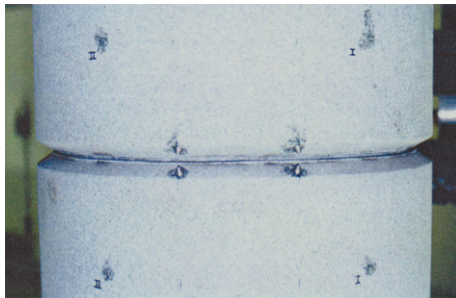


Fig. 5. Demec markers used for mated alignment of the fractured segments of the cylinder and measurement of the initial aperture width.

was absent, the fracture plane could be nonplanar, which presents an obstacle for inducing pure compression on the fracture plane. The splitting test generally produced a relatively planar fracture with some evidence of compression failure near the point of applications of the loads. This result is, however, not the norm, and on occasions, the fracture surfaces can deviate from the position of the groove; this can result in a warped fracture surface and can also lead to edge fractures. The surfaces of the fractures of the sample tested were cleared of debris and loose particles by air blowing prior to laser scanning of the surfaces. Laser scanning of the surfaces was conducted at the *Center for Intelligent Machines* at McGill University. Laser scanning was used as a visual guide to establish the topography of the fracture and for assessing any damage to the surface during axial compression. The scanning accuracy of the

laser device was approximately 0.1 mm. The surface topography is shown in Fig. 6. The fracture does not display any dominant features that would negate the use of the parallel plate model.

The re-assembled sample was placed in the testing machine, and LVDTs were installed to measure the reduction in the fracture aperture width during application of compressive stresses. A reservoir collected the fluid migrating through the fracture during attainment of a steady flow rate. The outlet of the reservoir was maintained at approximately the level of the fracture plane.

### EXPERIMENTAL PROCEDURES AND RESULTS

The fracture was subjected to axial stresses and constant flow rates varying from 0.1 to 10 ml min<sup>-1</sup> were maintained to achieve steady flow conditions depending on the level of axial stress and the resulting aperture closure. Altogether, three loading-unloading cycles were performed on the fracture and the permeability of the fracture was calculated using Equation (5). Fig. 7 illustrates the closure of the fracture during application of the axial normal stress  $\sigma_n$ . The initial width of the fracture aperture  $2\lambda_0 \approx 0.0707$  mm. The fracture exhibits significant closure during the first cycle of loading up to 2.5 MPa. At the peak load of 7.5 MPa, applied during the third cycle of loading, the fracture aperture reduces to  $(2\lambda)_{\min} \approx 0.0022$  mm. Upon complete unloading of the fracture in the third cycle, the residual fracture aperture of

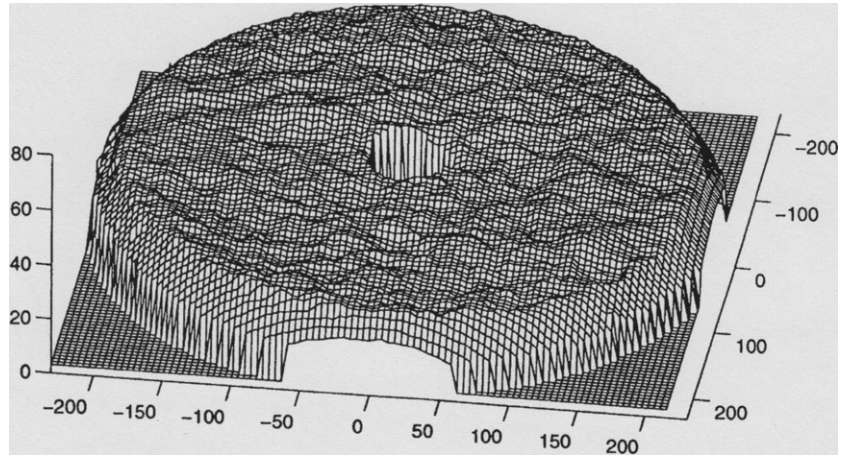


Fig. 6. The fracture surface topography [All dimensions are in mm].

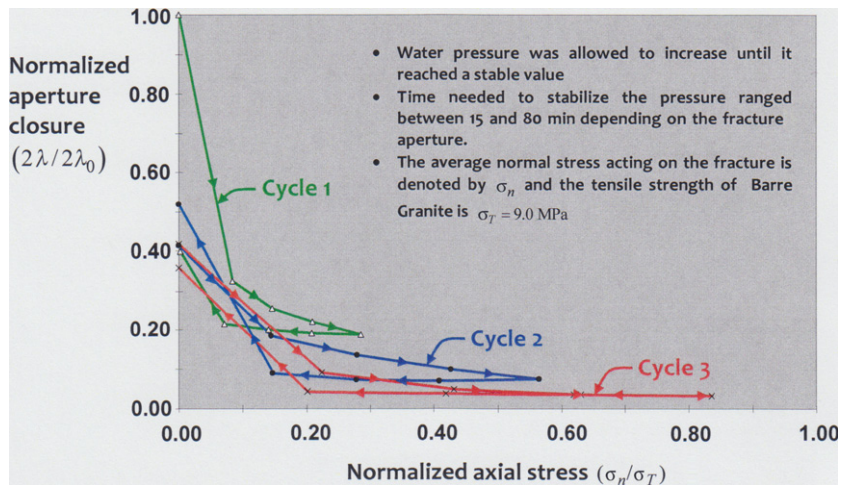


Fig. 7. Fracture closure during application of normal stresses. [It should be noted that the starting position of the fracture during cycle 3 does not coincide with the end position of cycle 2. This is most likely due to unloading effects and the release of elastic strain energy in the system. The discrepancy, however, does not affect the third cycle of loading and the aperture closure trend with increasing axial stress is consistent with that observed in cycles 1 and 2.]

$(2\lambda)_{res} \approx 0.0321$  mm. Figure 8 illustrates the variation in the permeability of the fracture during three loading-unloading cycles of applied axial stress  $\sigma_n$ . The first cycle of loading was performed by subjecting the fracture to a maximum normal stress of 2.5 MPa. At this level of axial stress, the flow rates need to be increased to approximately  $10 \text{ ml min}^{-1}$  to ensure an accurate measurement of fluid pressure within the cylindrical cavity. The experiments were repeated for two other cycles of loading and unloading where the peak stresses were 5.0 MPa and 7.5 MPa. At larger axial stresses, the lower flow rate of  $0.1 \text{ ml min}^{-1}$  was sufficient to develop accurately measurable pressures within the central cavity. The first cycle of axial loading establishes a reduction in permeability that persists for subsequent load cycles despite the apparent absence of mechanical alteration of the fracture during the loading-unloading cycles. The permeability of the fracture reduces from approximately  $1.0 \times 10^{-10} \text{ m}^2$  to  $1.2 \times 10^{-13} \text{ m}^2$  over the axial stress range zero to 7.5 MPa. In theory, axial stresses could be further increased, but the maximum stresses achievable are governed by both the capacity of the loading device and the tensile strength of the granite. With

increasing axial stress on half of the sample a tensile fracture developed, similar to those that can occur in a Brazilian Test.

In the experiment, the parameters that are measured are the pressure in the cylindrical cavity and the flow rate. The permeability of the fracture can be calculated by either

- 1 Including the flow through both the fracture and the intact matrix (Equation [5])

or

- 2 By assuming that the flow takes place in the fracture only (Equation [8]). Because an estimate of permeability of the intact matrix is available from hydraulic pulse tests conducted previously (Selvadurai *et al.* 2005), it is possible to examine the combined influences of axial stresses on the fracture and permeability of the matrix on the interpretation of the fracture permeability.

Table 1 presents results that consider the two theoretical estimates outlined by (i) and (ii) and indicates the relative error associated with the two estimates. As the normal stress acting on the fracture increases, omission of the component of flow through the intact matrix can lead to errors in the estimation of the permeability of the fracture.

**Table 1** Estimates for the permeability of a fracture in a Barre Granite cylinder during normal stress-induced fracture aperture reduction

Loading cycle	Maximum		Permeability Estimate (8)	Overestimation of fracture permeability
	Normal stress	Permeability Estimate (5)		
	$(\sigma_n)$	$(K_f^I)$	$(K_f^{II})$	$\left(\frac{K_f^{II}-K_f^I}{K_f^I}\right)$
1	2.5 MPa	$2.33 \times 10^{-11} \text{ m}^2$	$2.33 \times 10^{-11} \text{ m}^2$	0%
2	5.0 MPa	$3.37 \times 10^{-12} \text{ m}^2$	$3.43 \times 10^{-12} \text{ m}^2$	1.78%
3	7.5 MPa	$1.95 \times 10^{-13} \text{ m}^2$	$4.10 \times 10^{-13} \text{ m}^2$	102%

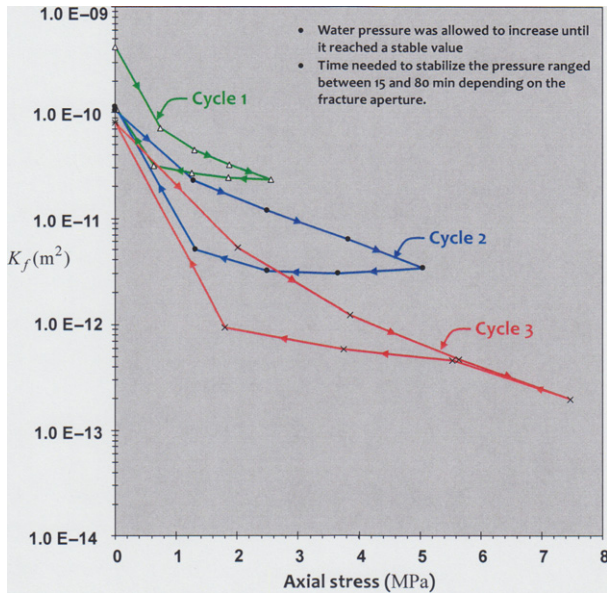


**Fig. 8.** Evolution of the permeability of the fracture during quasi-static application of loading-unloading cycles.

The assessment of heterogeneity of fracture permeability is an important topic (Boulon 1995; Armand 2000; Giacomini *et al.* 2007), but requires a detailed sensing of fluid flow patterns both within the fracture and at the outer boundaries. After the series of axial compression cycles, the surfaces of the fracture were scanned and superposed to assess asperity degradation during pure axial stressing. The results of the laser scanning are shown in Fig. 9 with colours indicating the level of mismatch. Red and purple colours indicate the level of strong mismatch that is expected at the boundary of the V-groove, and the points at which loads were applied to fracture the specimen. The blue colour indicates a perfect match between the two surfaces, and the yellow colour indicates a mismatch that is accurate to within 0.1 mm. There is no major deterioration of the mated fracture during axial compression.

**CONCLUDING REMARKS**

The paper presents the results of a series of permeability tests conducted on cylinders of intact and fractured Barre Granite. The intact permeability measured via pulse tests

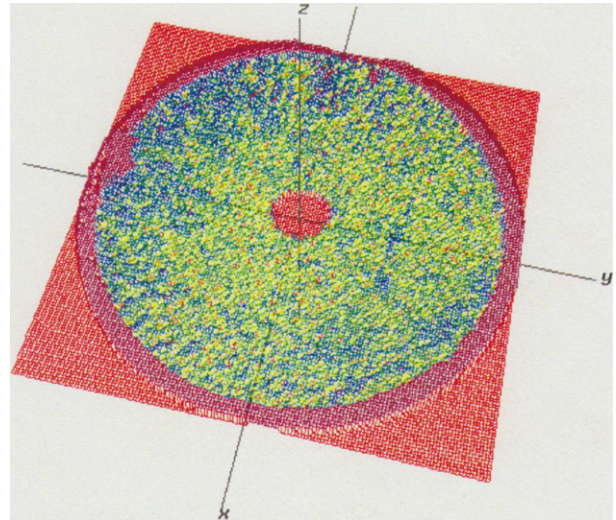


**Fig. 9.** Fracture topography mismatch after three cycles of axial compression normal to the plane of the fracture to a maximum stress of 7.5 MPa.

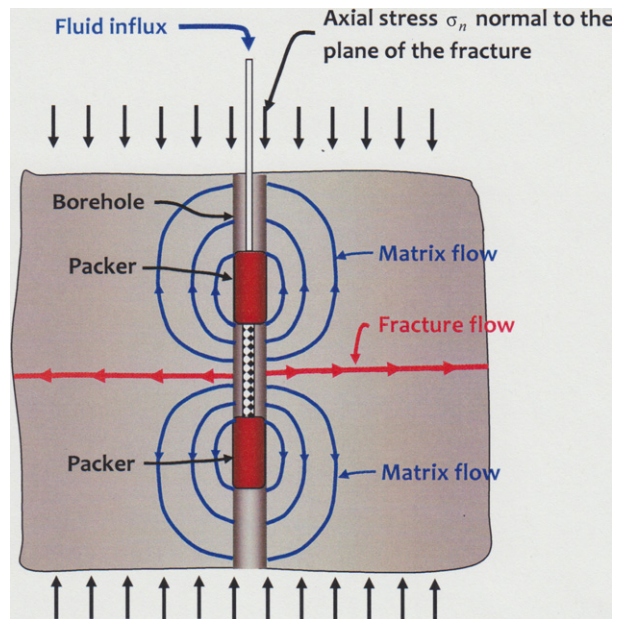


**Fig. 10.** Leakage through the matrix region during fracture permeability testing using a double packer system.

provides a basis to accurately interpret the permeability of a cylindrical specimen containing a plane fracture subjected to normal stress. The range of axial stresses applied to the fracture is indicative of geostatic stresses that can be present in shallow earth environments (<100 m), and as such, the results are of particular interest to geomechanical and groundwater resources applications. Reduction of the *in situ* normal stress acting on a fracture to zero, for example by either excavation or stress relief, can result in a permeability increase of around three orders of magnitude. The tests were conducted on a mated set of fracture surfaces,

which is representative of fractures unaffected by shearing action. The relatively large scale of the experiments is relevant to interpreting the hydro-mechanical performance of near surface fractures. For *in situ* permeability measurements of fractures at significant crustal depths, the conventional procedure is to employ packer systems to estimate the permeability. At significant depths, it is entirely possible that the fractures can remain tight owing to the *in situ* stress conditions, so that flow through the tight fracture can be comparable to leakage from the intact zone (Fig. 10). If the flow through the matrix is not accounted for, this will lead to an erroneous interpretation of the permeability of the fracture (Table 1). This effect will also be important for more highly permeable materials, such as sandstone and limestone where the intact permeability can approach that of the fracture at normal stress levels well within those required to induce diametral splitting of a fractured specimen. The aperture closure during the application of axial stresses exhibits hysteresis during the three loading-unloading cycles. The hysteretic behaviour is characteristic of interfaces that can consist of mated surfaces but with the possibility of displaying frictional phenomena at the scale of the asperities [Selvadurai & Boulon 1995; Selvadurai and Nguyen, 1997; Nguyen & Selvadurai 1998; Massart and Selvadurai, 2012, 2014]. This is a complex interface process where asperities can deform at contact points but release the elastic energy to create frictional unloading that can lead to a persistent hysteresis until the asperities experience damage and failure.

## ACKNOWLEDGEMENTS

The work described in the paper was supported by a research contract awarded by the Canadian Nuclear Safety Commission, Ottawa, Canada and through a Discovery Grant awarded by the Natural Sciences and Engineering Research Council of Canada. The author is grateful to the reviewers for their highly constructive comments that led to significant improvements in the presentation. The work was carried out in the Environmental Geomechanics Laboratory of the Department of Civil Engineering and Applied Mechanics at McGill University. The author acknowledges the support of the researchers at CNSC, in particular Dr. T. S. Nguyen, and the technical assistance of Mr. Nick Vannelli, Engineer and Mr. John Bartczak, Departmental Technician is greatly appreciated.

## REFERENCES

Adler PM (1997) Fracture deformation and influence on permeability. *Physical Review*, **56**, 3167–84.  
 Armand G (2000) *Contribution à la caractérisation en laboratoire et à la modélisation constitutive du comportement mécanique des joints rocheux*, Thesis, Université Joseph Fourier, Grenoble, France.

Bandis S, Lumsden AC, Barton NR (1983) Fundamentals of rock joint deformation. *International Journal of Rock Mechanics and Mining Sciences & Geomechanics Abstracts*, **20**, 249–68.  
 Bart M, Shao JF, Lydzba D, Haji-Sotoudeh M (2004) Coupled hydromechanical modeling of rock fractures under normal stress. *Canadian Geotechnical Journal*, **41**, 686–97.  
 Barton N (1982) *Modelling Rock Joint Behaviour From in Situ Block Tests: Implication for Nuclear Waste Repository Design*. Office of Nuclear Waste Isolation, Columbus, Ohio, ONWI-308, 96 pp.  
 Barton N, Choubey V (1977) The shear strength of rock joints in theory and practice. *Rock Mechanics*, **10**, 1–54.  
 Bear J (1972) *Dynamics of Fluids in Porous Media*. American Elsevier, New York.  
 Benjelloun ZH (1993) *Étude Expérimentale et Modélisation du Comportement Hydromécanique des Joints Rocheux*, Thèse de doctorat, Université Joseph Fourier, Grenoble.  
 Biot MA (1941) General theory of three-dimensional consolidation. *Journal of Applied Physics*, **12**, 155–64.  
 Boulon MJ (1995) A 3-D direct shear device for testing the mechanical behaviour and the hydraulic conductivity of rock joints, *Proceedings of the MJFR-2 Conference Vienna*, Austria, Balkema, Rotterdam, 407–413.  
 Boulon MJ, Selvadurai APS, Benjelloun H, Feuga B (1993) Influence of rock joint degradation on hydraulic conductivity. *International Journal of Rock Mechanics and Mining Sciences and Geomechanics Abstracts*, **30**, 1311–17.  
 Chan T, Christiansson R, Boulton GS, Ericsson LO, Hartikainen J, Jensen MR, Mas Ivars D, Stanchell FW, Vistrand P, Wallroth T (2005) DECOVALEX III BMT 3/BENCHPAR WP4: The thermo-hydro-mechanical responses to a glacial cycle and their potential implications for deep geological disposal of nuclear fuel waste in a fractured crystalline rock mass. *International Journal of Rock Mechanics and Mining Sciences*, **42**, 805–27.  
 Cook NGW (1992) Jaeger memorial dedication lecture: natural joints in rock: Mechanical, hydraulic and seismic behaviour and properties under normal stress. *International Journal of Rock Mechanics and Mining Sciences and Geomechanics Abstracts*, **29**, 198–223.  
 Elliot GM, Brown ET, Boodt PI, Hudson JA (1985) Hydrochemical behaviour of joints in the Carmenelis granite SW England, *Proceedings of the International Symposium on Fundamentals of Rock Joints*, Bjorkliden, Sweden, A. A. Balkema, Rotterdam, 249–258.  
 Gale J (1990) Hydraulic behaviour of rock joint, *Conference on Rock Joints, Proceedings of the ISRM*, 351–362.  
 Giacomini A, Buzzi O, Ferrero AM, Migliazza M, Giani GP (2007) Numerical study of flow anisotropy within a single natural rock joint. *International Journal of Rock Mechanics and Mining Sciences*, **45**, 47–58.  
 Haimson BC (1975) The state of stress in the Earth's crust. *Reviews of Geophysics*, **13**, 350–2. doi:10.1029/RG013i003p00350 (<http://dx.doi.org/10.1029/RG013i003p00350>).  
 Hans J, Boulon MJ (2003) A new device for investigating the hydro-mechanical properties of rock joints. *International Journal for Numerical and Analytical Methods in Geomechanics*, **27**, 513–48.  
 Hardy JR Jr (1991) *Laboratory Tests Conducted on Barre Granite: Compressive Strength, Flexural Strength, Modulus of Rupture, Adsorption and Bulk Specific Gravity and Petrographic Analysis*. Department of Mining Engineering, Pennsylvania State University, PA.

- Hu DW, Zhu QZ, Zhou H, Shao JF (2010) A discrete approach for anisotropic plasticity and damage in semi-brittle rocks. *Computational Geotechnics*, **37**, 658–66.
- Hudson JA, Bäckström A, Rutqvist J, Jing L (2008) DECOVALEX-THMC Project. Task B Understanding and characterizing the excavation disturbed zone, Final Report (EDZ Guidance Document) Characterizing and Modelling the Excavation damaged Zone (EDZ) in Crystalline Rocks in the Context of Radioactive Waste Disposal, SKI Report 43.
- Ichikawa Y, Selvadurai APS (2012) *Transport Phenomena in Porous Media: Aspects of Micro/Macro Behaviour*. Springer Verlag, Berlin.
- Ingebritsen SE, Sanford W, Neuzil CE (2006) *Groundwater in Geologic Processes*. 2nd edn. Cambridge University Press, Cambridge. 536 p.
- Jaeger JC (1971) Friction of rocks and stability of rock slopes. *Geotechnique*, **21**, 97–134.
- Jafari MK, Pellet F, Boulon MJ, Amini Hosseini K (2004) Experimental study of mechanical behaviour of rock joints under cyclic loading. *Rock Mechanics and Rock Engineering*, **37**, 3–23.
- Kiyama T, Kita H, Ishijima Y, Yanagidani T, Akoi K, Sato T (1996) Permeability in anisotropic granite under hydrostatic compression and tri-axial compression including post-failure region, *Proceedings 2nd North American Rock Mechanics Symposium*, pp. 1643–50.
- Ladanyi B, Archambault G (1970) Simulation of Shear Behaviour of a Jointed Rock Mass, *Proceedings 11th Symposium on Rock Mechanics*. American Institute of Mechanical Engineers, New York.
- Liu H-H, Wei M-Y, Rutqvist J (2013) Normal-stress dependence of fracture hydraulic properties including two-phase flow properties. *Hydrogeology Journal*, **21**, 371–82.
- Louis C (1974) Rock hydraulics. In: *Rock Mechanics* (ed Muller L), pp. 299–387. Springer, Vienna.
- Mahyari AT, Selvadurai APS (1998) Enhanced consolidation in brittle geomaterials susceptible to damage. *Mechanics of Cohesive Frictional Materials*, **3**, 291–303.
- Makurat A, Barton N, Rad NS, Bandis S (1990a) Joint conductivity variation due to normal and shear deformation, *Proceedings International Symposium on Rock Joints*, Loen, Norway. Barton N, Stephansson O, eds. Balkema, Rotterdam, The Netherlands, 535–40.
- Makurat A, Barton N, Tunbridge L, Vik G (1990b) The measurements of the mechanical and hydraulic properties of rock joints at different scale in the Stripa project. *Proceedings of the International Symposium on Rock Joints*, Loen, Norway. Barton N, Stephansson O, eds. Balkema, Rotterdam, The Netherlands, 541–8.
- Massart TJ, Selvadurai APS (2012) Stress-induced permeability evolution in quasi-brittle geomaterials. *Journal of Geophysical Research (Solid Earth)*, **117**. doi:10.1029/2012JB009251.
- Massart TJ, Selvadurai APS (2014) Computational modelling of crack-induced permeability evolution in granite with dilatant cracks. *International Journal of Rock Mechanics and Mining Sciences*, **70**, 593–604.
- Méheust Y, Schmittbuhl J (2003) Flow enhancement of a rough fracture. *Pure and Applied Geophysics*, **160**, 1023–50.
- Najari M, Selvadurai APS (2014) Thermo-hydro-mechanical response of granite to temperature changes. *Environmental Earth Sciences*, **72**, 189–198.
- Nguyen TS, Jing L (2008) (Ed) *DECOVALEX-THMC Project. Task A. Influence of near field coupled THM phenomena on the performance of a spent fuel repository*. Report of Task A2, SKI Report 44, pp 1–100.
- Nguyen TS, Selvadurai APS (1995) Coupled thermal-mechanical-hydrological behaviour of sparsely fractured rock: implications for nuclear fuel waste disposal. *International Journal of Rock Mechanics and Mining Sciences and Geomechanics Abstracts*, **32**, 465–79.
- Nguyen TS, Selvadurai APS (1998) A model for coupled mechanical and hydraulic behaviour of a rock joint. *International Journal for Numerical and Analytical Methods in Geomechanics*, **22**, 29–48.
- Noorshad J, Tsang CF, Witherspoon PA (1984) Coupled thermo-hydraulic-mechanical phenomena in saturated fractured porous rocks: numerical approach. *Journal of Geophysical Research*, **89**, 10365–73.
- Patton FD (1966) Multiple modes of shear failure in rock, *Proceedings 1st Congress of International Society of Rock Mechanics. Lisbon*, **1**, 509–13.
- Philips OM (1991) *Flow and Reactions in Permeable Media*. Cambridge University Press, Cambridge.
- Plesha ME (1987) Constitutive models for rock discontinuities with dilatancy and surface degradation. *International Journal for Numerical and Analytical Methods in Geomechanics*, **11**, 345–362.
- Pyrak-Nolte LJ, Morris JP (2000) Single fractures under normal stress: the relation between fracture specific stiffness and fluid flow. *International Journal of Rock Mechanics and Mining Sciences*, **37**, 245–62.
- Raven KG, Gale JE (1985) Water flow in a natural rock fracture as a function of stress and sample size. *International Journal of Rock Mechanics and Mining Sciences and Geomechanics Abstracts*, **22**, 251–61.
- Rejeb A, Rouabhi A, Millard A, Maßmann J, Uehara S (2008) *DECOVALEX-THMC Project. Task C Hydromechanical response of the Tournemire Argillite to the underground openings excavation: unsaturated zones and mine-by-test experiment*. Final Report, SKI Report, 44, 1–100.
- Rutqvist J, Tsang C-F (2002) A study of caprock hydromechanical changes associated with CO<sub>2</sub> injection into a brine formation. *Environmental Geology*, **42**, 296–305.
- Rutqvist J, Freifeld B, Min K-B, Elsworth D, Tsang Y (2008) Analysis of thermally induced changes in fractured rock permeability during eight years of heating and cooling at the Yucca Mountain Drift Scale Test. *International Journal of Rock Mechanics and Mining Sciences*, **45**, 1373–89.
- Sausse J, Genter A (2005) Types of permeable fractures in granite. *Geological Society of London, Special Publications*, **240**, 1–14.
- Selvadurai APS (1996) (Ed.) *Mechanics of Poroelastic Media*. Kluwer Academic Publishers, The Netherlands.
- Selvadurai APS (2000) *Partial Differential Equations in Mechanics Vol. I: Fundamentals, Laplace's Equation, the Diffusion Equation, the Wave Equation*. Springer-Verlag, Berlin, 595 pp. [Special Edition released in Peoples Republic of China, 2004].
- Selvadurai APS (2004) Stationary damage modelling of poroelastic contact. *International Journal of Solids and Structures*, **41**, 2043–64.
- Selvadurai APS (2007) The analytical method in geomechanics. *Applied Mechanics Reviews*, **60**, 87–106.
- Selvadurai APS (2009) Fragmentation of ice sheets during impact. *Computer Modeling in Engineering and Science*, **52**, 259–77.
- Selvadurai APS, Boulon MJ (1995) (Eds.) *Mechanics of Geomaterial Interfaces*. Studies in Applied Mechanics, Vol. 42, Elsevier Scientific Publishers, The Netherlands.
- Selvadurai APS, Carnaffan P (1997) A transient pressure pulse technique for the measurement of permeability of a cement grout. *Canadian Journal of Civil Engineering*, **24**, 489–502.

- Selvadurai APS, Głowacki A (2008) Evolution of permeability hysteresis of Indiana Limestone during isotropic compression. *Ground Water*, **46**, 113–19.
- Selvadurai APS, Ichikawa Y (2013) Some aspects of air-entrainment on decay rates in hydraulic pulse tests. *Engineering Geology*, **165**, 38–45.
- Selvadurai APS, Jenner L (2012) Radial flow permeability testing of an argillaceous limestone. *Ground Water*, **51**, 100–107.
- Selvadurai APS, Najari M (2013) On the interpretation of hydraulic pulse tests on rock specimens. *Advances in Water Resources*, **53**, 139–49.
- Selvadurai APS, Nguyen TS (1995) Computational modeling of isothermal consolidation of fractured porous media. *Computers and Geotechnics*, **17**, 39–73.
- Selvadurai APS, Nguyen TS (1997) Scoping analyses of the coupled thermal-hydrological-mechanical behaviour of the rock mass around a nuclear fuel waste repository. *Engineering Geology*, **47**, 379–400.
- Selvadurai APS, Selvadurai PA (2010) Surface permeability tests: Experiments and modelling for estimating effective permeability, Proceedings of the Royal Society. *Mathematics and Physical Sciences Series A*, **466**, 2819–2846.
- Selvadurai APS, Sepehr K (1999a) Discrete element modelling of fragmentable geomaterials with size dependent strength. *Engineering Geology*, **53**, 235–41.
- Selvadurai APS, Sepehr K (1999b) Two dimensional discrete element simulation of ice–structure interaction. *International Journal of Solids and Structures*, **36**, 4919–40.
- Selvadurai APS, Shirazi A (2004) Mandel-Cryer effects in fluid inclusions in damage susceptible poroelastic media. *Computers and Geotechnics*, **37**, 285–300.
- Selvadurai APS, Shirazi A (2005) An elliptical disc anchor in a damage-susceptible poroelastic medium. *International Journal of Numerical Methods in Engineering*, **16**, 2017–39.
- Selvadurai APS, Yu Q (2005) Mechanics of a discontinuity in a geomaterial. *Computers and Geotechnics*, **32**, 92–106.
- Selvadurai APS, Yue ZQ (1994) On the indentation of a poroelastic layer. *International Journal of Numerical and Analytical Methods in Geomechanics*, **18**, 161–75.
- Selvadurai APS, Boulon MJ, Nguyen TS (2005) The permeability of an intact granite. *Pure and Applied Geophysics*, **162**, 373–407.
- Selvadurai APS, Letendre A, Hekimi B (2011) Axial flow hydraulic pulse testing of an argillaceous limestone. *Environmental Earth Sciences*, **64**, 2047–2058.
- Shao JF, Hoxha D, Bart M, Homand F, Duveau G, Souley M, Hoteit N (1999) Modelling of induced anisotropic damage in granites. *International Journal of Rock Mechanics and Mining Science*, **36**, 1001–12.
- Shiping L, Yushou L, Yi L, Zhenye W, Gang Z (1994) Permeability-strain equations corresponding to the complete stress–strain path of Yin Zhuang Sandstone. *International Journal of Rock Mechanics and Mining Sciences and Geomechanics Abstracts*, **31**, 383–91.
- Snow DT (1968) Rock fracture spacings, openings, and porosities. *Journal of the Soil Mechanics and Foundations Division, ASCE*, **94**, 73–91.
- Souley M, Homand F, Pepa S, Hoxha D (2001) Damage-induced permeability changes in granite: a case example at the URL in Canada. *International Journal of Rock Mechanics and Mining Science*, **38**, 297–310.
- Stephansson O (Ed.) (1985) *Proceedings of the International Symposium on Fundamentals of Rock Joints*. Bjökliden, Norway.
- Wang H (2000) *Theory of Linear Poroelasticity with Applications to Geomechanics and Hydrogeology*. Princeton University Press, Princeton, NJ.
- Witherspoon P, Amick C, Gale J, Iwai K (1979) Observation of a potential size effect in experimental determination of the hydraulic properties of fractures. *Water Resources Research*, **15**, 1142–6.
- Yeo IW, de Freitas MH, Zimmermann RW (1998) Effect of shear displacement on the aperture and permeability of a rock fracture. *International Journal of Rock Mechanics and Mining Sciences*, **35**, 1051–70.
- Zhou JJ, Shao JF, Xu WY (2006) Coupled modeling of damage growth and permeability variation in brittle rocks. *Mechanics Research Communications*, **33**, 450–9.
- Zhu W, Wong TF (1997) The transition from brittle faulting to cataclastic flow: permeability evolution. *Journal of Geophysical Research*, **102**, 3027–41.
- Zoback MD, Byerlee JD (1975) The effect of micro-crack dilatancy on the permeability of Westerly Granite. *Journal of Geophysical Research*, **80**, 752–5.

# GEOFLUIDS

Volume 15, Number 1 and 2, February 2015

ISSN 1468-8115

## CONTENTS

### INTRODUCTION TO THE SPECIAL ISSUE ON CRUSTAL PERMEABILITY

- 1 Crustal permeability: Introduction to the special issue**  
*S.E. Ingebritsen and T. Gleeson*

### THE PHYSICS OF PERMEABILITY

- 11 A pore-scale investigation of the dynamic response of saturated porous media to transient stresses**  
*C. Huber and Y. Su*
- 24 Flow of concentrated suspensions through fractures: small variations in solid concentration cause significant in-plane velocity variations**  
*R. Medina, J.E. Elkhoury, J.P. Morris, R. Prioul, J. Desroches and R.L. Detwiler*
- 37 Normal stress-induced permeability hysteresis of a fracture in a granite cylinder**  
*A.P.S. Selvadurai*
- 48 Fractured rock stress-permeability relationships from in situ data and effects of temperature and chemical-mechanical couplings**  
*J. Rutqvist*

### STATIC PERMEABILITY

#### *Sediments and sedimentary rocks*

- 67 How well can we predict permeability in sedimentary basins? Deriving and evaluating porosity-permeability equations for noncemented sand and clay mixtures**  
*E. Luijendijk and T. Gleeson*
- 84 Evolution of sediment permeability during burial and subduction**  
*H. Daigle and E.J. Screaton*

#### *Igneous and metamorphic rocks*

- 106 Is the permeability of crystalline rock in the shallow crust related to depth, lithology or tectonic setting?**  
*M. Ranjram, T. Gleeson and E. Luijendijk*
- 120 Understanding heat and groundwater flow through continental flood basalt provinces: insights gained from alternative models of permeability/depth relationships for the Columbia Plateau, USA**  
*E.R. Burns, C.F. Williams, S.E. Ingebritsen, C.I. Voss, F.A. Spane and J. Deangelo*
- 139 Deep fluid circulation within crystalline basement rocks and the role of hydrologic windows in the formation of the Truth or Consequences, New Mexico low-temperature geothermal system**  
*J. Pepin, M. Person, F. Phillips, S. Kelley, S. Timmons, L. Owens, J. Witcher and C. Gable*
- 161 Hydraulic conductivity of fractured upper crust: insights from hydraulic tests in boreholes and fluid-rock interaction in crystalline basement rocks**  
*I. Stober and K. Bucher*

### DYNAMIC PERMEABILITY

#### *Oceanic crust*

- 179 Rapid generation of reaction permeability in the roots of black smoker systems, Troodos ophiolite, Cyprus**  
*J.R. Cann, A.M. McCaig and B.W.D. Yardley*

#### *Fault zones*

- 193 The permeability of active subduction plate boundary faults**  
*D.M. Saffer*
- 216 Changes in hot spring temperature and hydrogeology of the Alpine Fault hanging wall, New Zealand, induced by distal South Island earthquakes**  
*S.C. Cox, C.D. Menzies, R. Sutherland, P.H. Denys, C. Chamberlain and D.A.H. Teagle*
- 240 The where and how of faults, fluids and permeability – insights from fault stepovers, scaling properties and gold mineralisation**  
*S. Micklethwaite, A. Ford, W. Witt and H.A. Sheldon*
- 252 Evidence for long timescale ( $>10^3$  years) changes in hydrothermal activity induced by seismic events**  
*T. Howald, M. Person, A. Campbell, V. Lueth, A. Hofstra, D. Sweetkind, C.W. Gable, A. Banerjee, E. Luijendijk, L. Crossey, K. Karlstrom, S. Kelley and F.M. Phillips*

#### *Crustal-scale-behaviour*

- 269 An analytical solution for solitary porosity waves: dynamic permeability and fluidization of nonlinear viscous and viscoplastic rock**  
*J.A.D. Connolly and Y.Y. Podladchikov*
- 293 Hypocenter migration and crustal seismic velocity distribution observed for the inland earthquake swarms induced by the 2011 Tohoku-Oki earthquake in NE Japan: implications for crustal fluid distribution and crustal permeability**  
*T. Okada, T. Matsuzawa, N. Umino, K. Yoshida, A. Hasegawa, H. Takahashi, T. Yamada, M. Kosuga, T. Takeda, A. Kato, T. Igarashi, K. Obara, S. Sakai, A. Saiga, T. Iidaka, T. Iwasaki, N. Hirata, N. Tsumura, Y. Yamanaka, T. Terakawa, H. Nakamichi, T. Okuda, S. Horikawa, H. Katao, T. Miura, A. Kubo, T. Matsushima, K. Goto and H. Miyamachi*
- 310 Continental-scale water-level response to a large earthquake**  
*Z. Shi, G. Wang, M. Manga and C.-Y. Wang*

#### *Effects of fluid injection at the scale of a reservoir or ore deposit*

- 321 Development of connected permeability in massive crystalline rocks through hydraulic fracture propagation and shearing accompanying fluid injection**  
*G. Preisig, E. Eberhardt, V. Gischig, V. Roche, M. Van Der Baan, B. Valley, P.K. Kaiser, D. Duff and R. Lowther*
- 338 Modeling enhanced geothermal systems and the essential nature of large-scale changes in permeability at the onset of slip**  
*S.A. Miller*
- 350 The dynamic interplay between saline fluid flow and rock permeability in magmatic-hydrothermal systems**  
*P. Weis*

### A DATA STRUCTURE TO INTEGRATE AND EXTEND EXISTING KNOWLEDGE

- 372 DigitalCrust – a 4D data system of material properties for transforming research on crustal fluid flow**  
*Y. Fan, S. Richard, R.S. Bristol, S.E. Peters, S.E. Ingebritsen, N. Moosdorf, A. Packman, T. Gleeson, I. Zaslavsky, S. Peckham, L. Murdoch, M. Fioren, M. Cardiff, D. Tarboton, N. Jones, R. Hooper, J. Arrigo, D. Gochis, J. Olson and D. Wolock*